INFECTION AND IMMUNITY, Feb. 2011, p. 674–687 Vol. 79, No. 2
0019-9567/11/$12.00 doi:10.1128/IAI.00808-10

Distinct CCR2$^+$ Gr1$^+$ Cells Control Growth of the *Yersinia pestis* Δ*yopM* Mutant in Liver and Spleen during Systemic Plague▽†

Zhan Ye,[1] Annette M. Uittenbogaard,[1] Donald A. Cohen,[1] Alan M. Kaplan,[1] Jayakrishna Ambati,[2] and Susan C. Straley[1]*

Department of Microbiology, Immunology, and Molecular Genetics[1] *and Department of Ophthalmology and Visual Sciences,*[2] *University of Kentucky, Lexington, Kentucky 40536-0298*

Received 23 July 2010/Returned for modification 4 September 2010/Accepted 1 December 2010

We are using a systemic plague model to identify the cells and pathways that are undermined by the virulence protein YopM of the plague bacterium *Yersinia pestis*. In this study, we pursued previous findings that Gr1$^+$ cells are required to selectively limit growth of Δ*yopM Y. pestis* and that CD11b$^+$ cells other than polymorphonuclear leukocytes (PMNs) are selectively lost in spleens infected with parent *Y. pestis*. When PMNs were ablated from mice, Δ*yopM Y. pestis* grew as well as the parent strain in liver but not in spleen, showing that these cells are critical for controlling growth of the mutant in liver but not spleen. In mice lacking expression of the chemokine receptor CCR2, wild-type growth was restored to Δ*yopM Y. pestis* in both organs. In spleen, the Gr1$^+$ cells differentially recruited by parent and Δ*yopM Y. pestis* infections were CCR2$^+$ Gr1$^+$ CD11b$^+$ CD11c$^{Lo\text{-}Int}$ MAC3$^+$ iNOS$^+$ (inducible nitric oxide synthase-positive) inflammatory dendritic cells (iDCs), and their recruitment to spleen from blood was blocked when YopM was present in the infecting strain. Consistent with influx of iDCs being affected by YopM in spleen, the growth defect of the Δ*yopM* mutant was relieved by the parent *Y. pestis* strain in a coinfection assay in which the parent strain could affect the fate of the mutant in *trans*. In a mouse model of bubonic plague, CCR2 also was shown to be required for Δ*yopM Y. pestis* to show wild-type growth in skin. The data imply that YopM's pathogenic effect indirectly undermines signaling through CCR2. We propose a model for how YopM exerts its different effects in liver and spleen.

A major virulence property of the plague bacterium *Yersinia pestis* is a set of 6 protein toxins that are delivered directly into host cells through a contact-dependent type III secretion system (T3SS) (62). Five of the Yops disrupt signaling through small GTPases within host cells, with consequent inhibition of phagocytosis and downregulation of production of proinflammatory cytokines that are important for activation of macrophages (Mϕs) and development of adaptive immunity (59, 62). All of the Yops counteract innate defenses, but YopM is the only one lacking a proposed enzymatic mechanism that clearly links its molecular action to its pathogenic effect (59, 62). YopM is a highly acidic 409-residue protein comprised of a leader sequence involved in recognition and delivery through the T3SS, 15 leucine-rich repeats (LRRs), and a short C-terminal tail sequence. The enteropathogenic yersiniae *Y. pseudotuberculosis* and *Y. enterocolitica* have a T3SS and a set of Yops that are highly similar to those in *Y. pestis*. However, of the Yops, YopM is the most variable in sequence, containing from 13 to 21 LRRs. YopM has no sequence similarity to any known enzymes, and because the majority of its structure consists of LRRs which are known to function as protein-protein interaction motifs, YopM is viewed as a scaffold that potentially can assemble novel signaling complexes (35).

YopM is required for full lethality of *Y. pestis* in systemic plague initiated by intravenous (i.v.) infection and in bubonic plague after intradermal (i.d.) infection but not in pneumonic plague following intranasal infection (25, 30, 66). In systemic plague, the bacteria seed liver and spleen within 30 min (6). By day 2 postinfection (p.i.), *Y. pestis* lacking YopM evidences slower growth in these organs; concomitantly, lower net levels of mRNA for proinflammatory cytokines are detected in liver and spleen of mice infected with the parent strain than in organs of mice infected with a Δ*yopM* mutant (25). Expression of mRNA for tumor necrosis factor alpha (TNF-α), interleukin-1β (IL-1β), IL-12, IL-15, IL-18, and gamma interferon (IFN-γ), cytokines that activate innate immune cells, including Mϕs, dendritic cells (DCs), natural killer (NK) cells, and polymorphonuclear leukocytes (PMNs), is greatly decreased by day 4 p.i. in mice infected with the parent strain of *Y. pestis* compared to that in mice infected by the Δ*yopM* mutant, which show a continued robust inflammatory response (25). Subsequently, the Δ*yopM* mutant begins to be cleared from organs (25, 30).

YopM distributes between the cytoplasm and the nucleus of infected cells, and its nuclear localization depends upon functional vesicular trafficking, implying that YopM likely makes multiple interactions within cells and could have multiple pathogenic effects (53). Ruter et al. (46) recently showed that YopM contains a pair of motifs in its N-terminal leader region that could sponsor autonomous cell penetration of the protein in a caveola-dependent manner. After internalization in HeLa cells, YopM initially localized to early endosomes, moved to late endosomes and the perinuclear region, and eventually reached the endoplasmic reticulum and nucleus without passing through the Golgi apparatus. When HL60 cell-derived

* Corresponding author. Mailing address: Department of Microbiology, Immunology, and Molecular Genetics, University of Kentucky, Lexington, KY 40536-0298. Phone: (859) 323-6538. Fax: (859) 257-8994. E-mail: scstra01@uky.edu.

† Supplemental material for this article may be found at http://iai.asm.org/.

▽ Published ahead of print on 13 December 2010.

TABLE 1. Bacterial strains and plasmids used in this study

Strain or plasmid	Relevant properties	Source or reference
Y. pestis strains		
KIM5	Pgm$^-$ Lcr$^+$ pCD1 pMT1 pPCP1; conditionally virulent Δ*pgm* 2.MED strain; also called KIM D27	R. R. Brubaker
KIM5-3003	Δ*lacZ* derivative of KIM5; 1.2 kb of *lacZ* coding sequence deleted by allelic exchange with pLacZ3	This study
CO92.S6	CO92 Ap^r Pgm$^+$ Lcr$^+$ pFra pPCP1; reconstituted virulent strain made by introduction of pCD2Ap into CO92.S1	12
CO92.S19	Reconstituted Lcr$^+$ Δ*yopM2* strain made by introducing pCD2Ap Δ*yopM2* from CO99-3015.S11 into CO92.S1	66
E. coli strain		
DH5αλ*pir*	*recA1 endA1 gyrA96 thi-1 hsdR17 supE44 relA1deoR* Δ(*lacZYA-argF*)*U169* λ*pir*$^+$; host strain for maintaining pLacZ3	Lab stock
Plasmid		
pLacZ3	Suicide allelic exchange plasmid for transferring internal 1.2-kb deletion into *Y. pestis lacZ*; 12.8 kb, R6K origin, SucB$^+$ Sm^r Δ*lacZ*	4

macrophages were treated with YopM and then with lipopolysaccharide (LPS) for 16 h, the same proinflammatory cytokines that are downregulated *in vivo* (25) showed inhibited mRNA expression (except IFN-γ, which was not tested). Neither Kerschen et al. nor Ruter et al. found the level of mRNA for IL-10 to be increased by YopM.

Several proteins have been identified as being able to bind YopM: α-thrombin (30), α1-antitrypsin (19), and the serine/threonine kinases RSK1 and PRK2, which as a consequence become activated (34–36). McPhee et al. (36) studied i.v. infection by *Y. pseudotuberculosis* and linked the presence of the immunosuppressive cytokine IL-10 in serum of mice on day 4 with expression of a YopM identical to that of *Y. pestis*. IL-10 was not present in serum of mice infected with *Y. pseudotuberculosis* that expressed a variant of YopM that lacked the C terminus and the last three LRRs and was unable to bind RSK1 or a YopM variant that lacked the majority of the protein (LRRs 6 to 15) and was unable to bind PRK2 but still bound RSK1. McCoy et al. identified two molecular complexes that contained YopM and RSK1, localized the binding site for RSK1 to the last 6 residues in the YopM tail, and showed that substitution mutations altering these residues caused a decreased ability of *Y. pseudotuberculosis* to inhibit recruitment of monocytes (MOs) and to colonize spleen and lung. These findings implicate RSK1 as a potential molecular target of YopM. However, the pathway from RSK1 to YopM's effects on cytokine expression during infection (25, 36) has not yet been delineated. Moreover, because the interaction of YopM with RSK1 did not account for the full effect of YopM on virulence of *Y. pseudotuberculosis*, it remains likely that YopM makes multiple interactions within host cells that may have pathogenic consequences.

Our lab has been using the systemic plague model to identify the immunologic steps at which YopM has its earliest effects and then to work back to the associated signaling pathways affected by YopM. In i.v.-infected C57BL/6 mice, the growth limitation on Δ*yopM Y. pestis* in liver and spleen provides a strong YopM-specific virulence phenotype that greatly facilitates sorting out the key players in YopM's pathogenic effects. This growth difference stems from a defect in the ability of *Y. pestis* to counteract innate defenses when YopM is absent (25). Our approach to discovering how YopM functions is to identify the host defenses that impose this defect specifically or disproportionately on the Δ*yopM* mutant compared to the parent *Y. pestis* strain that contains YopM. Previously, we found that Gr1$^+$ cells (PMNs, MOs, and some DCs) are required to impose the growth defect: in mice depleted of these cells, Δ*yopM Y. pestis* grows as well as the parent strain in both liver and spleen (66). There also is a striking YopM-associated loss of NK cells in spleens (but not livers) of mice infected with parent *Y. pestis* (25, 66). NK cells are not required to limit growth of Δ*yopM Y. pestis* (66), but the effect of YopM on NK cells provides a marker for how YopM alters host responses in spleen.

In this study, we sought to identify the Gr1$^+$ cells that are responsible for limiting *Y. pestis* growth in liver and spleen in systemic plague. We found that the relevant cells differed, with inflammatory DCs (iDCs) mediating the effect in spleen and PMNs mediating the effect in liver, reflecting the distinct antibacterial responses of the two organs. In these cells, the chemokine receptor CCR2 was required in different ways for controlling the growth of Δ*yopM Y. pestis*. In the case of iDCs, CCR2 was required to recruit these cells. The data also provided a likely basis for the effect of YopM on NK cells, because these cells also depend on signaling through CCR2 for recruitment.

MATERIALS AND METHODS

Bacterial strains and *in vitro* cultivation. Bacterial strains and plasmids used in this study are listed in Table 1. The *Y. pestis* strains represent the two most recently evolved groups of *Y. pestis* populations (1): *Y. pestis* KIM5 (molecular grouping 2.MED), an isolate from Iran, and *Y. pestis* CO92 (1.ORI), isolated in the United States. *Y. pestis* KIM5 and the Δ*yopM1* derivative KIM5-3002 lack the chromosomal *pgm* locus and are conditionally virulent: they are attenuated from peripheral routes of infection but are virulent by the i.v. route of infection, which bypasses the requirement for a siderophore-based iron acquisition mechanism encoded in this locus (60). *Y. pestis* CO92.S6 is fully virulent, and *Y. pestis* CO92.S19 is an isogenic Δ*yopM2* mutant (66). Herein, these isogenic pairs of strains are designated parent and Δ*yopM* strains (note that the parent strains are not true wild types [WT], because of the antibiotic resistance marker in pCD2Ap of CO92 and the Δ*pgm* mutation in KIM). The Δ*lacZ Y. pestis* strain KIM5-3003 was created in the *Y. pestis* KIM5 background by allelic exchange followed by sucrose selection to cure the suicide plasmid pLacZ3 as described previously (4).

Escherichia coli was grown in Luria-Bertani broth or agar (37) at 37°C. *Y. pestis*

KIM5-derived strains were routinely grown at 26°C in heart infusion broth (HIB; Difco Laboratories) and harvested in exponential phase at A_{620} of 0.8 to 1.2. Cells were centrifuged at 23,281 × *g* and 4°C for 5 min, washed, and diluted in phosphate-buffered saline (PBS). Samples from the dilutions were plated on tryptose blood agar (Difco Laboratories) and incubated at 30°C for 2 days to determine the actual dose. *Y. pestis* CO92-derived strains were grown at 28°C in HIB supplemented with 2.5 mM $CaCl_2$, 0.2% xylose, and 50 μg/ml carbenicillin (Cb). The cultures were diluted in PBS before being used to infect mice. Samples of the doses and appropriate serial dilutions were plated on supplemented HIB, and the number of CFU was determined after incubation for 2 days at 28°C. The presence of the pigmentation locus (43) in all Pgm^+ strains was confirmed by the formation of red colonies on Congo red agar (58) at 28°C.

Infection of mice and measurement of bacterial viable numbers in tissues. All animal experiments in this study were reviewed and approved by the University of Kentucky Institutional Animal Care and Use Committee. Mice used were 6- to 8-week-old female C57BL/6N.HSD mice (Harlan Sprague Dawley, Inc.) and female $CCR2^{-/-}$ and $CCL2^{-/-}$ C57BL/6J mice (2) ranging from 6 to 15 weeks of age. For studies with *Y. pestis* KIM5, KIM5-3002, and KIM5-3003, mice were anesthetized with an isoflurane-oxygen mixture by a rodent anesthesia machine. Fifty microliters (400 CFU) of bacterial suspension was injected i.v. via the retroorbital plexus. This dose was above the 50% lethal dose (LD_{50}) for the parent strain and below that for the Δ*yopM1* mutant. The two bacterial strains grow similarly for the initial 24 h of infection (references 25 and 66 and this study [see Fig. 1]); accordingly, the innate host responses were elicited by similar bacterial numbers, and differences were due to the presence or absence of YopM and not to nonspecific factors. At designated times after infection, groups of mice were humanely killed by CO_2 inhalation followed by cervical dislocation, and their spleens and livers were weighed, transferred to a sterile bag containing 5 ml of PBS, and homogenized in a Stomacher 80 lab blender (Tekmar Co.). The liver and spleen homogenates were diluted in PBS and plated to measure viable bacterial numbers (CFU) in the organs. In some experiments, blood also was obtained by cardiac puncture using a syringe containing 30 μl of heparin solution (1,000 U/ml; Elkins-Sinn, Inc.). Approximately 200 μl of blood from each mouse was mixed with 5 ml of PBS. The mixture was carefully overlaid over 5 ml Lympholyte-Mammal medium (Cedarlane Labs) and then centrifuged at 600 × *g* for 20 min at room temperature. The leukocytes were obtained from the interface and washed twice in PBS containing 1% (wt/vol) bovine serum albumin and 0.1% (wt/vol) sodium azide (PBS-BSA-azide).

For infection with *Y. pestis* CO92 strains, the mice were shaved on the back at the base of the tail and anesthetized with ketamine (100 mg/kg of body weight; IVX Animal Health) and xylazine (10 mg/kg; Butler Co.) given intraperitoneally (i.p.). Bacterial doses were made in 100 μl of PBS and injected i.d. with a 1-ml tuberculin syringe fitted with a retractable 26-gauge needle (Becton Dickinson and Company). The effect of xylazine was then reversed by subcutaneous injection of yohimbine (2 mg/kg; Ben Venue Laboratories) on the back of the neck, and the mice were treated with an optical lubricant before being returned to their cages. At day 4 or 5 p.i., the mice were humanely killed by i.p. injection of 100 μl of Beuthanasia-D (solution containing pentobarbital sodium and phenytoin sodium [Schering-Plough]) followed by thoracic puncture, and the spleen and a patch of skin surrounding the infection site were recovered. Spleens were minced and taken into a 3-ml syringe along with 1 ml of sterile water. A second syringe equipped with a 20-gauge emulsifying needle was attached, and the sample was passed back and forth 20 times to further disrupt the tissue and release the bacteria. The piece of skin was minced and transferred to a 50-ml conical tube containing 2 ml of a sterile solution of PBS, collagenase (40,000 U/ml), dispase protease (224 U/ml), and DNase (16,000 U/ml). The tubes were then agitated for 30 min in an upright position at 250 rpm on a gyrotory platform at 37°C. The resulting digest was taken into a 5-ml syringe and emulsified as described above through an 18-gauge emulsifying needle. The resulting spleen and skin suspensions were then serially diluted in PBS and plated in duplicate to determine CFU.

Innate immune cell ablation. Mice were given a PMN-specific anti-Ly6G monoclonal antibody (MAb 1A8; Bio X Cell) i.p. at 200 μg/mouse on days −1 and +1 of *Y. pestis* infection to ablate PMNs. Mock-treated control mice received rat IgG (Sigma) at the same dose and schedule. The extent of ablation in these and in mock-treated mice was assessed by flow cytometry with detection via fluorochrome-tagged anti-Ly6G and anti-CD11b antibodies (see below).

Flow cytometry. Leukocytes were analyzed in a FACSCalibur flow cytometer (Becton Dickinson and Company) as described previously (66). Briefly, homogenized spleens were centrifuged and resuspended in 2 ml red blood cell (RBC) lysis buffer (150 mM NH_4Cl, pH 7.2). After 2 min, the reaction was terminated by addition of 8 ml of PBS. The cell suspensions were filtered through a 40-μm-pore-size cell strainer (Becton Dickinson and Company), centrifuged, and resuspended in PBS-BSA-azide. Minced livers in 10 ml RPMI 1640 (Life Technologies Inc.) with 10% fetal bovine serum (FBS) (ATCC) were processed with the Stomacher 80 lab blender. The homogenates were incubated with DNase I (160 U/ml; Sigma-Aldrich) and collagenase (400 U/ml; Invitrogen) for 30 min at 37°C, with shaking at 125 rpm. After filtration through a 40-μm-pore-size cell strainer, cell suspensions were washed once with ice-cold PBS-BSA-azide and resuspended with 5 ml 33.8% Percoll (Amersham Bioscience), followed by centrifugation. The cells in the bottom layer were collected, washed with PBS, treated with RBC lysis buffer, and resuspended in PBS-BSA-azide.

The following antibodies were purchased from BD Pharmingen, Inc.: allophycocyanin (APC)-conjugated anti-CD11c, fluorescein isothiocyanate (FITC)-conjugated anti-CD11b, FITC-conjugated anti-inducible nitric oxide synthase (iNOS), phycoerythrin (PE)-conjugated anti-Ly6G, PE-conjugated anti-CD11b, PE-conjugated anti-TNF-α, PE-conjugated anti-Mac3, peridinin chlorophyll protein-cyanine 5.5 (PerCP Cy5.5)-conjugated anti-Gr1, and Fc block (rat anti-mouse CD16 and CD32). PE-conjugated donkey anti-rabbit IgG and nonconjugated rabbit anti-mouse CCR2 were purchased from Abcam. Nonspecific rat IgG was obtained from Sigma. Ethidium monoazide (EMA; Sigma) was used for viability staining.

Prior to staining, the cells were counted, and samples were adjusted to 5×10^6 cells per ml. They were stained as described previously (66). Briefly, after treatment with Fc block for 15 min on ice, the cells were incubated with appropriate combinations of antibodies and EMA on ice for 30 min, with the last 10 min of incubation in the light. They were then washed in PBS and resuspended in ice-cold PBS containing 4% (wt/vol) paraformaldehyde (pH 7.4) for at least 30 min before flow cytometric analysis.

To detect intracellular iNOS, TNF-α, and Mac3 in particular cell types, cells were processed with a BD Cytofix/Cytoperm Plus fixation/permeabilization kit (BD Biosciences). Briefly, cells were treated with GolgiPlug (1 μl per 10^6 cells in 1 ml of cell suspension) for 4 h at 37°C followed by surface marker staining as described above. Then, the cells were incubated with fixation/permeabilization solution for 20 min at 4°C. After being washed with Perm/Wash buffer, the cells were stained with appropriate antibodies at 4°C for 1 h in the dark and then washed and resuspended in PBS-BSA-azide for flow cytometric analysis.

Flow cytometric processing was performed by the Flow Cytometry Core Facility at the University of Kentucky. The data were analyzed with WinMDI (version 2.7; Joseph Trotter, Salk Institute for Biological Studies, La Jolla, CA [available at http://facs.Scripps.edu/software.html]). EMA-positive apoptotic or dead cells were gated out, and total live leukocytes (EMA-negative cells) were analyzed further for surface and intracellular staining. The total numbers of live leukocytes in spleen and liver did not differ in mice infected with the two *Y. pestis* strains at the times p.i. that were analyzed in detail (days 1, 2, and 3) (see Table S1 in the supplemental material). Accordingly, it was valid to express the flow cytometry data as the percentage of total live leukocytes.

Statistical analysis. Infection experiments with flow cytometric and CFU analyses were conducted at least twice with at least 3 replicate mice per group, typically resulting in 6 to 9 mice per datum point. In two cases (the experiments with results shown in Fig. 1 and 6), previously obtained data could be reanalyzed and pooled with data taken in this study, resulting in large numbers of mice per datum point and increased statistical power. The data from the replicate experiments were pooled, and significance of differences among groups was assessed by Student's unpaired 2-tailed *t* test. *P* values of <0.05 were considered significant. Data are presented as mean values ± standard deviations (SD), and the numbers of mice used for each datum point are given in the figure legends. Pairwise comparison of data groups with nonparametric distributions was made with the Wilcoxon two-sample test.

RESULTS

PMNs are not essential for limiting growth of Δ*yopM Y. pestis* in spleen but are essential in liver. This study used a well-characterized i.v. infection model in which liver and spleen are seeded by *Y. pestis* within 30 min (6). Because YopM is required for full lethality of bubonic plague initiated by i.d. infection (66), we grew the yersiniae at 26°C to enable us to identify innate defenses that specifically control growth of a Δ*yopM* strain that initially was not adapted to mammalian body temperature, as would be the case upon delivery of *Y. pestis* to the dermis by flea bite. Figure 1A illustrates the growth phenotypes of the Δ*yopM* mutant and the parent strain

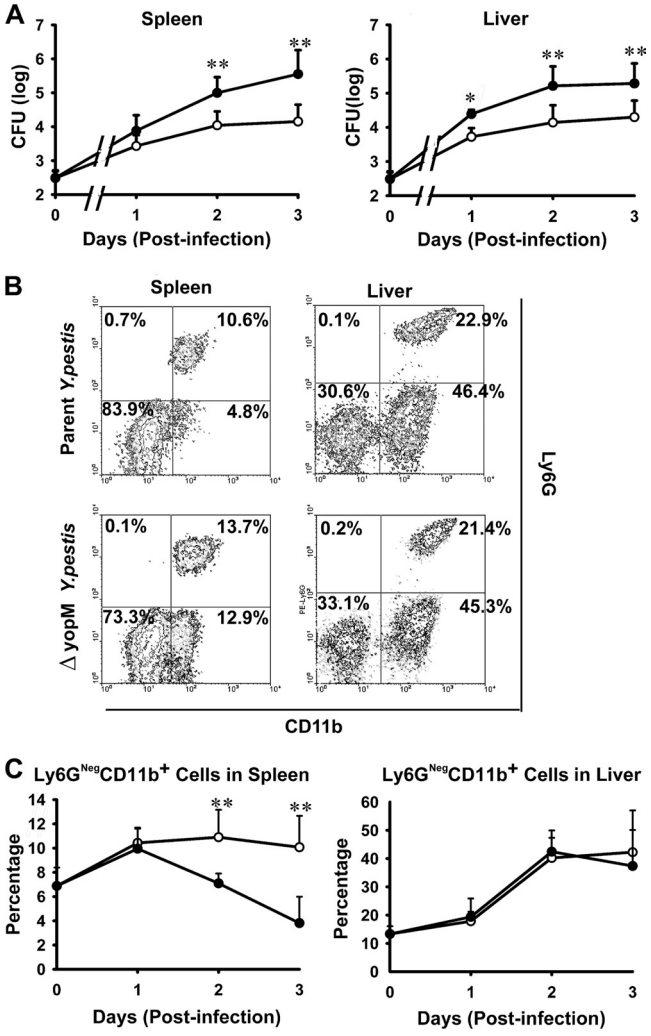

FIG. 1. Infection dynamics for Δ*yopM* and parent *Y. pestis* KIM5. C57BL/6 mice were infected i.v. with 400 bacteria that had been grown at 26°C. At the indicated times, groups of mice were analyzed for bacterial viable numbers (CFU) in liver and spleen, and populations of live leukocytes in liver and spleen were distinguished by flow cytometry. (A) CFU in spleens and livers of mice infected with parent (filled circles) or Δ*yopM* (open circles) *Y. pestis* KIM5. The point at time zero indicates the dose given to the mice. (B) Flow cytometric scatter plots illustrating the discrimination of populations of live leukocytes for the presence of Ly6G and CD11b surface markers. Representative data are shown for leukocytes from liver and spleen of an individual mouse infected with parent or Δ*yopM Y. pestis* on day 3 p.i. The percentage of total live leukocytes contained in each quadrant is given. (C) $Ly6G^-$ ($Ly6G^{Neg}$) $CD11b^+$ cells (MOs, Mϕs, and myeloid DCs) expressed as percentage of total live leukocytes in spleens and livers of mice infected with the parent (filled circles) or the Δ*yopM* (open circles) strain. The point at time zero indicates the value for uninfected mice. In panels A and C, each datum point represents the average of values from 26 mice. The error bars indicate the standard deviations. Significant differences by unpaired Student's *t* test comparing data from mice infected with the parent and mutant strains are indicated (*, $P < 0.05$; **, $P < 0.01$).

in C57BL/6 mice infected i.v. with 400 bacteria. As seen previously (25, 66), the mutant grew more slowly than the parent strain as early as day 1 p.i.

In our previous study, we found that the growth difference between mutant and parent *Y. pestis* was eliminated when the mice had been treated with anti-granulocyte receptor 1 (Gr1) antibody. This antibody recognizes cross-reacting epitopes on two surface molecules: Ly6G, which is specific for PMNs, and Ly6C, which is present on PMNs and subsets of monocytes, DCs, and lymphocytes. This result indicated that one or more types of $Gr1^+$ (i.e., $Ly6G^+$ and/or $Ly6C^+$) cells must be directly or indirectly counteracted by YopM. One prominent candidate cell is the PMN, which is abundant and able to phagocytose and kill *Y. pestis* (56). To test the possibility that PMNs preferentially limit growth of the Δ*yopM* strain, we treated mice with antibody that recognizes only the PMN-specific Ly6G surface marker (9) on the day before and the day after infection to ablate PMNs without reducing numbers of other $Gr1^+$ cells. Viable bacterial numbers and populations of live inflammatory cells were measured in liver and spleen on days 2 and 3 p.i. (Fig. 2 for day 3 p.i. and data not shown for day 2). The ablation reduced PMN numbers by 86 to 92% in spleens and by 95 to 97% in livers compared to levels for mock-treated mice (data not shown) but had no effect on numbers of Δ*yopM* mutant bacteria in spleens (Fig. 2A), indicating that PMNs are not critical for selectively limiting growth of Δ*yopM Y. pestis* in spleen. However, in livers, the ablation eliminated the growth difference between parent and mutant strains and restored the wild-type growth yield to the Δ*yopM* mutant. This finding indicates that in liver, PMNs are largely responsible for the growth disadvantage of the Δ*yopM* mutant compared to parent *Y. pestis* and are cells whose function is directly or indirectly counteracted by YopM in the parent strain.

As noted previously (66), significantly greater numbers of $Ly6G^-$ $CD11b^+$ cells (Mϕs, MOs, and some DCs) were stably recruited to spleens in mice from which PMNs had not been ablated when YopM was absent in the infecting strain (Fig. 1B and C). This effect was not observed in livers, which showed identical accumulations of these cells during infection by both *Y. pestis* strains. Previously, we observed that ablation of $Gr1^+$ cells abolished the influx into infected spleens and delayed influx until day 3 p.i. in livers (66). However, ablation of only PMNs did not abolish or even decrease influx of $Ly6G^-$ $CD11b^+$ cells in either organ (Fig. 2B and C). This finding shows that PMNs are not essential for recruitment of these cells from the bone marrow and peripheral circulation into infected organs. Further, either a $Gr1^+$ cell other than PMNs is responsible for recruiting the $Ly6G^-$ $CD11b^+$ cells in response to infection or the recruited $Ly6G^-$ $CD11b^+$ cells themselves are $Gr1^+$ (by virtue of having the Ly6C surface molecule).

CCR2 is necessary for recruiting $Ly6G^-$ $CD11b^+$ cells into *Y. pestis*-infected spleens and livers. $Gr1^+$ microbicidal cells other than PMNs that migrate to sites of inflammation include inflammatory MOs (iMOs) and inflammatory DCs (iDCs), which develop from iMOs (11, 13, 50). These both express the C-C chemokine receptor CCR2 and are recruited into inflammatory foci predominantly by the chemokine CCL2 (also called monocyte chemotactic protein 1 [MCP-1]) (13), which binds to CCR2. In mice lacking CCR2 expression, iMOs and iDCs are defective for migration into foci of inflammation (5, 13, 49). PMNs may express CCR2 (22) but do not rely on this receptor for recruitment (5, 27, 61). Mice lacking CCR2 ex-

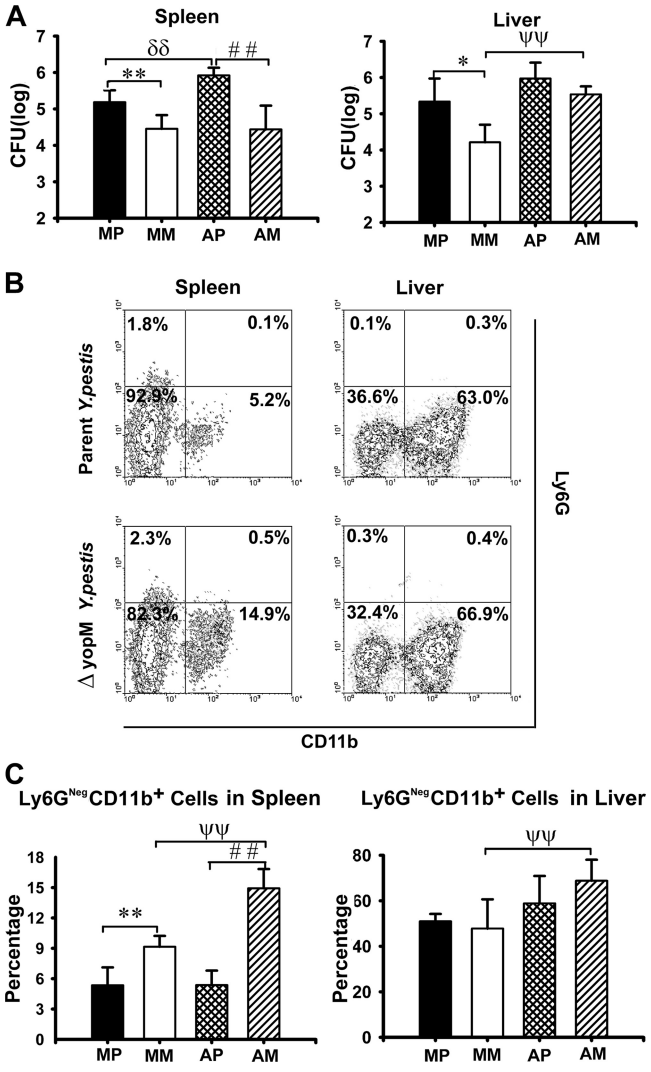

FIG. 2. Effect of PMN ablation on infection dynamics for Δ*yopM* and parent *Y. pestis* KIM5. Mice were treated with rat anti-Ly6G antibody to ablate PMNs, and control animals were mock treated with irrelevant (nonspecific) rat IgG on days −1 and +1 of infection. The mice were infected and analyzed as described in the legend for Fig. 1 for bacterial burdens and inflammatory leukocyte populations in livers and spleens on day 3 p.i. MP, mock-treated mice infected with parent *Y. pestis*; MM, mock-treated mice infected with the Δ*yopM* mutant; AP, PMN-ablated mice infected with the parent; AM, PMN-ablated mice infected with the Δ*yopM* mutant strain. (A) CFU. (B) Flow cytometric scatter plots illustrating the discrimination of populations of live leukocytes in anti-Ly6G-treated mice for the presence of Ly6G and CD11b surface markers. Representative data are shown for leukocytes from liver and spleen of individual mice infected with parent or Δ*yopM Y. pestis* (day 3 p.i.). The percentage of total live leukocytes contained in each quadrant is given. (C) Ly6G$^-$ CD11b$^+$ cells (MOs, Mϕs, and myeloid DCs) expressed as percentage of total live leukocytes. In panels A and C, each datum point represents the average of values from 6 mice. The error bars indicate the standard deviations. In comparisons between PMN ablation and mock ablation groups, ψψ, $P < 0.01$ for mice infected with the Δ*yopM* strain; δδ, $P < 0.01$ for mice infected with the parent strain. In comparisons between groups of mice infected with the parent and the Δ*yopM* strains, *, $P < 0.05$, and **, $P < 0.01$, for mock-treated mice; # #, $P < 0.01$ for PMN-ablated mice.

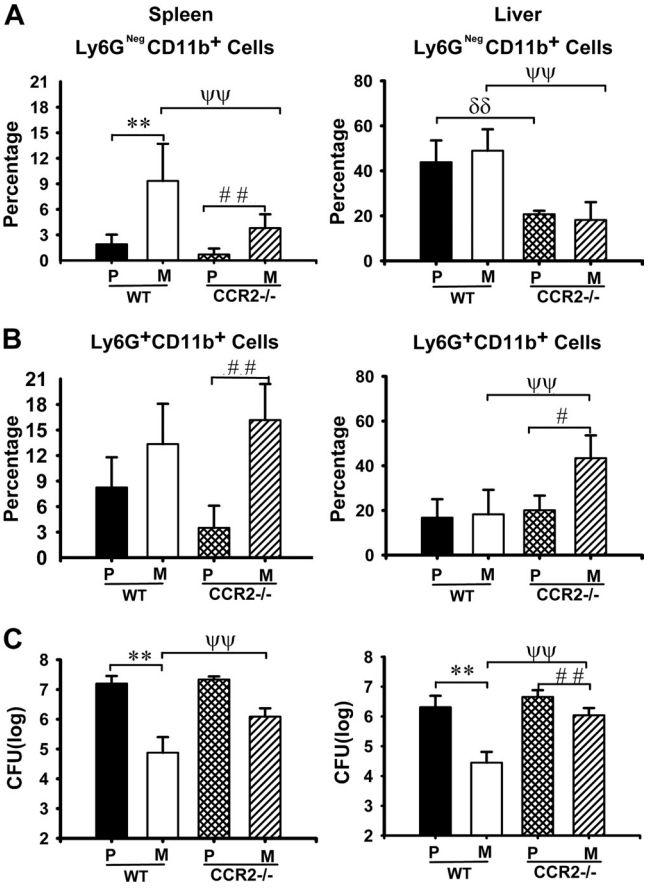

FIG. 3. CCR2 requirement for recruitment to selectively control growth of Δ*yopM Y. pestis* KIM5. WT and CCR2$^{-/-}$ C57BL/6 mice were infected and analyzed as described in the legend for Fig. 1 for bacterial burdens and inflammatory leukocyte populations in livers and spleens on day 3 p.i. P/WT, WT mice infected with parent *Y. pestis*; M/WT, WT mice infected with the Δ*yopM* mutant; P/CCR2$^{-/-}$, CCR2$^{-/-}$ mice infected with the parent strain; M/CCR2$^{-/-}$, CCR2$^{-/-}$ mice infected with the Δ*yopM* strain. Ly6G$^-$ CD11b$^+$ cells (MOs, Mϕs, and myeloid DCs) (A) and PMNs (Ly6G$^+$ CD11b$^+$ cells) (B) are expressed as percentage of total live leukocytes. (C) CFU. Each datum point represents the average of values from 9 mice. The error bars indicate the standard deviations. In comparisons between WT and CCR2$^{-/-}$ mice, ψψ, $P < 0.01$ for mice infected with the Δ*yopM* strain; δδ, $P < 0.01$ for mice infected with the parent strain. In comparisons between groups of mice infected with the Δ*yopM* and parent strains, **, $P < 0.01$ for WT mice; #, $P < 0.05$, and # #, $P < 0.01$, for CCR2$^{-/-}$ mice.

pression therefore allow us to test the importance of iMOs and iDCs in limiting the growth of Δ*yopM Y. pestis*, because these mice are defective in recruiting Gr1$^+$ iMOs and iDCs to *Y. pestis*-infected liver and spleen, whereas influx of PMNs can still occur. Other cells recruited via CCR2 are memory T cells and NK cells (10), but these cells are not Gr1$^+$ and are not required for controlling growth of Δ*yopM Y. pestis* (25, 66). Accordingly, we compared viable bacterial numbers and numbers of Ly6G$^-$ CD11b$^+$ leukocytes in livers and spleens of C57BL/6 (WT) and CCR2$^{-/-}$ mice infected with parent and Δ*yopM Y. pestis.* Figure 3A shows that there were significantly fewer of these cells in organs of CCR2$^{-/-}$ mice than in those of WT mice. As expected, the numbers were not completely

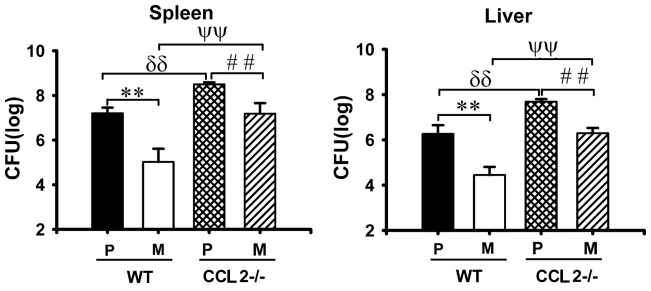

FIG. 4. Growth enhancement for both parent and Δ*yopM Y. pestis* KIM5 in mice lacking CCL2 (MCP-1). WT and CCL2$^{-/-}$ C57BL/6 mice were infected and analyzed as described in the legend for Fig. 1 for bacterial burdens on day 3 p.i. P/WT, WT mice infected with parent *Y. pestis*; M/WT, WT mice infected with the Δ*yopM* mutant; P/CCL2$^{-/-}$, CCL2$^{-/-}$ mice infected with the parent strain; M/CCL2$^{-/-}$, CCL2$^{-/-}$ mice infected with the Δ*yopM* strain. Each datum point represents the average of values from 9 mice. The error bars indicate the standard deviations. In comparisons between WT and CCL2$^{-/-}$ groups, ψψ, $P < 0.01$ for mice infected with the Δ*yopM* strain; δδ, $P < 0.01$ for mice infected with the parent strain. In comparisons between groups of mice infected with parent and Δ*yopM Y. pestis*, **, $P < 0.01$ for WT mice; # #, $P < 0.01$ for CCL2$^{-/-}$ mice.

abolished, because this grouping of surface markers includes resident Mϕs which are not CCR2$^+$, and some of the inflammatory Ly6G$^-$ CD11b$^+$ leukocytes might not strongly express CCR2 (see below). Also, although CCR2 is the major chemokine receptor for recruitment of iMOs and iDCs, some recruitment could occur via other chemokine receptors (10), and this could account for the residual differential recruitment into spleen in the CCR2$^{-/-}$ mice. The influx of PMNs was not significantly decreased in CCR2$^{-/-}$ mice, and in livers infected by Δ*yopM Y. pestis* there were even significantly increased numbers of PMNs (Fig. 3B). However, in the CCR2$^{-/-}$ mice, the growth restriction on the Δ*yopM* strain was significantly relieved, whereas growth of the parent strain was not affected (Fig. 3C). These data indicate that cells recruited or activated through CCR2 play a critical role in selectively limiting growth of Δ*yopM Y. pestis*.

In contrast to results for CCR2, parent and Δ*yopM Y. pestis* strains were similarly enhanced in growth in mice lacking a major ligand for CCR2, CCL2 (MCP-1), although the growth difference between the parent and Δ*yopM Y. pestis* strains was slightly decreased (Fig. 4). In these mice, CCR2$^+$ cells could still be recruited or activated via other ligands of CCR2, such as CCL7 (10, 24, 41).

Ly6G$^-$ Gr1$^+$ CD11b$^+$ cells that are differentially recruited in spleens infected with Δ*yopM* and parent *Y. pestis* are inflammatory DCs. The experiments so far had shown that in spleen, some Ly6G$^-$ CD11b$^+$ cells were differentially recruited during infection by Δ*yopM* and parent *Y. pestis*, that the numbers of these differentially recruited cells were diminished in CCR2$^{-/-}$ mice, and that concomitantly the growth limitation of the Δ*yopM* strain was significantly relieved. Taken together with our previous finding that Gr1$^+$ cells are required to limit growth of the Δ*yopM* strain (66), the simplest hypothesis was that the cells required to mediate the growth limitation in spleen were Gr1$^+$ CCR2$^+$ Ly6G$^-$ CD11b$^+$ cells that were differentially recruited via CCR2 into sites of infection by the Δ*yopM* and parent strains. The anti-Gr1 antibody recognizes two epitopes: Ly6G, specific for PMNs, and Ly6C, which is present on MOs, some DCs, and memory CD8$^+$ T cells as well as PMNs (9, 64). With the exception of PMNs, migration of these cells is controlled by CCR2. The likely CD11b$^+$ candidates for controlling bacterial growth early in infection were iMOs and iDCs. Therefore, we evaluated the dynamics of these cells in liver and spleen of WT and CCR2$^{-/-}$ mice after infection by parent and Δ*yopM Y. pestis*. We distinguished iDCs from iMOs by the level of CD11c expression, with iMOs being CD11c$^-$ and iDCs being CD11c^{Lo} or CD11c^{Int} (CD11c$^{Lo\text{-}Int}$) (51, 57). Because iMOs range in Ly6C expression from high to intermediate (57), this marker was not useful for distinguishing them from iDCs (which are Ly6C^{Hi} [50]). Both cell types express inducible nitric oxide synthase (iNOS) (50). Figure 5A illustrates these cell populations as separated by flow cytometry of live leukocytes from the spleen of mice infected with parent and Δ*yopM Y. pestis* on day 3 p.i. The demarcated region contains the CD11b$^+$ CD11c$^{Lo\text{-}Int}$ iDCs. The iDCs responding to *Listeria monocytogenes* infection were found to have high expression of TNF-α, iNOS, and CD107b (the membrane glycoprotein Mac3) and were named TipDCs (TNF-α-/iNOS-producing DCs) (51). The CD11b$^+$ CD11c$^{Lo\text{-}Int}$ cell population in spleens of mice infected with *Y. pestis* was highly enriched for cells strongly expressing these markers (Fig. 5B), with 85% being iNOS$^+$, 81% being TNF-α$^+$, and 83% being Mac3$^+$. Further, as expected, 85% of the CD11b$^+$ CD11c$^{Lo\text{-}Int}$ iDCs were Gr1$^+$, and the majority (64%) were CCR2$^+$ (Fig. 5B). Accordingly, the iDCs that respond to *Y. pestis* infection resembled TipDCs by these major markers.

The CD11b$^+$ CD11c$^{Lo\text{-}Int}$ iDCs showed a dramatic YopM-related difference in accumulation in *Y. pestis*-infected spleen but not in liver (Fig. 6). Further, when we gated out both PMN and iDC populations from the analyses of total CD11b$^+$ cells, the relative numbers of remaining CD11b$^+$ cells were the same for mice infected with parent and Δ*yopM* mutant strains, confirming that iDCs accounted for the preferential accumulation of CD11b$^+$ cells in spleens of WT mice infected with the Δ*yopM* mutant by day 2 p.i. (data not shown).

The main chemokine receptor known to govern migration of iMOs (the precursor cells of iDCs) is CCR2, and we hypothesized that the CD11b$^+$ cells preferentially recruited to spleens infected with Δ*yopM Y. pestis* would require CCR2 for their accumulation. Accordingly, we tested for the effect of CCR2 knockout on the population dynamics of iDCs during infection by comparing iDC numbers in spleens and livers of WT and CCR2$^{-/-}$ mice infected with parent and Δ*yopM Y. pestis*. As expected, the numbers of iDCs in spleens of CCR2$^{-/-}$ mice were greatly diminished compared to those in spleens of WT mice, and the YopM-associated differential recruitment of these cells was abolished (Fig. 7). However, the abundance of these cells in infected livers was only weakly affected by lack of CCR2 expression, indicating that in liver, chemokines other than those that signal through CCR2 can serve to recruit iDCs.

The data from Fig. 2B and C indicated that there is no YopM-related recruitment into liver of the Ly6G$^-$ CD11b$^+$ mixed population of cells. However, because we had found that PMNs play a role in controlling Δ*yopM Y. pestis* in liver, we wanted to confirm that PMNs are not involved in recruiting the iDC subset of cells into liver. These tests showed that depletion

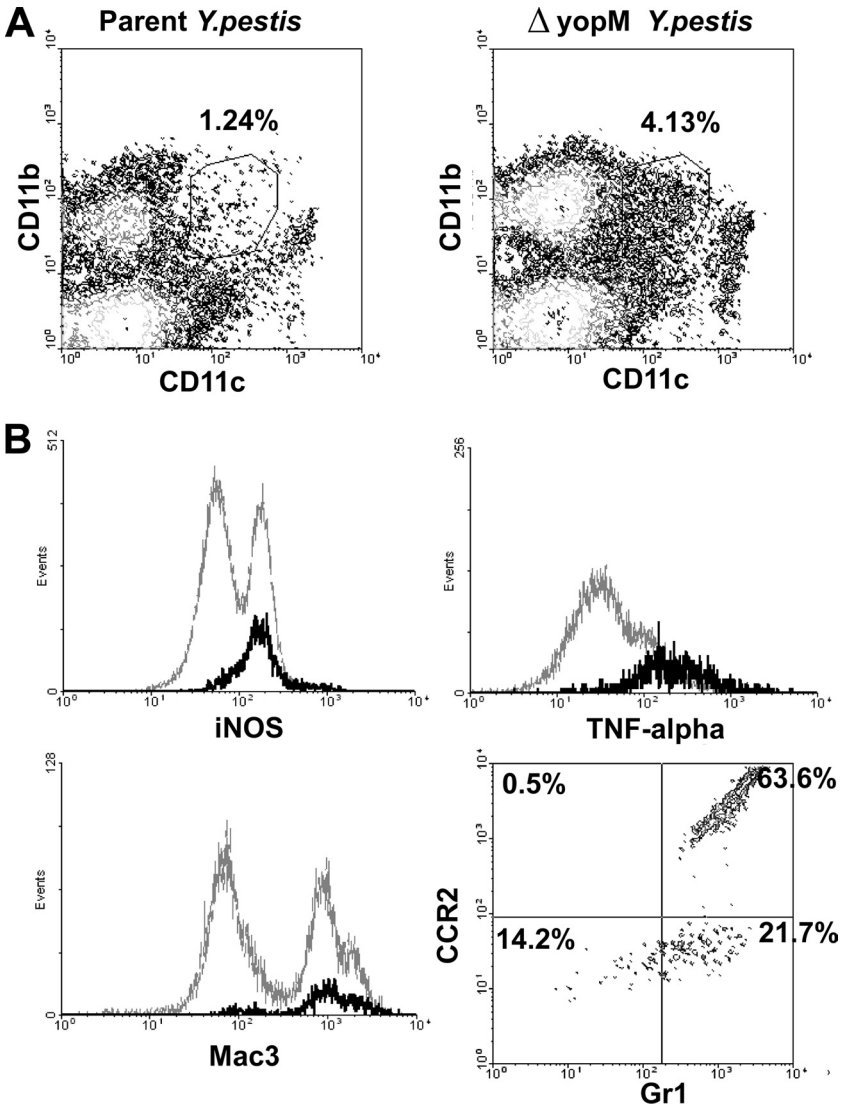

FIG. 5. Flow cytometric characterization of inflammatory dendritic cells preferentially recruited to spleens infected with Δ*yopM Y. pestis* KIM5. C57BL/6 mice were infected as described in the legend for Fig. 1 and analyzed for inflammatory leukocyte populations in spleens on day 3 p.i. (A) Flow cytometric scatter plots defining a population of $CD11b^+$ $CD11c^{Lo\text{-}Int}$ cells recruited to spleen of a mouse infected by parent or Δ*yopM Y. pestis* (demarcated by the surround). The percentage of total live leukocytes contained in the demarcated region is given. (B) Further flow cytometric characterization of the $CD11b^+$ $CD11c^{Lo\text{-}Int}$ cell population from spleen of an individual mouse infected with Δ*yopM Y. pestis*. The histograms compare intracellular staining for iNOS, TNF-α, and Mac3 in the $CD11b^+$ $CD11c^{Lo\text{-}Int}$ cell population (black) to that for the total live leukocytes (gray). The scatter plot shows the surface staining of $CD11b^+$ $CD11c^{Lo\text{-}Int}$ cells for Gr1 and CCR2.

of PMNs indeed had no effect on numbers of iDCs in either liver or spleen (see Fig. S1 in the supplemental material).

Taken together, the findings so far were consistent with the interpretation that iDCs constitute a critical inflammatory cell response to infection of spleens by 26°C-grown Δ*yopM Y. pestis* and that the parent strain with YopM in some way prevents the influx of these cells. The $CD11b^+$ $CD11c^{Lo\text{-}Int}$ iDCs are $Gr1^+$ and would have been depleted, along with PMNs, by the anti-Gr1 antibody treatment that relieved the growth limitation of the Δ*yopM* mutant (66). In mice with cells ablated by anti-Gr1 antibody, no $Ly6G^-$ $CD11b^+$ cells accumulated in spleens in response to infection by Δ*yopM Y. pestis* (66). Further, iDCs are $CCR2^+$ and were significantly diminished in recruitment into spleens in $CCR2^{-/-}$ mice, where the growth limitation of the Δ*yopM* mutant was significantly relieved. However, a different $Gr1^+$ CCR2-dependent cell must be critical for limiting growth of mutant *Y. pestis* in liver: although CCR2 knockout did selectively enhance growth of the Δ*yopM* strain in livers, CCR2 knockout only partially reduced the numbers of iDCs in livers, and these cells were not selectively recruited into livers infected by the Δ*yopM* mutant.

The parent *Y. pestis* initially inhibits recruitment of $Ly6G^-$ $CD11b^+$ cells into spleens from blood and subsequently also causes decreased numbers of these cells in blood. iDCs and iMOs both derive from MOs in bone marrow, and CCR2 functions in the recruitment of MOs from bone marrow into the circulation (49). iMOs home to infected tissues and extravasate, also guided by chemokines, including those that act

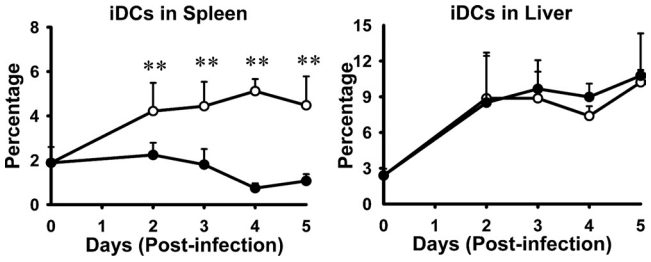

FIG. 6. Preferential recruitment of iNOS-producing CD11c$^{Lo\text{-}Int}$ CD11b^{+} iDCs to spleens infected with Δ*yopM Y. pestis* KIM5. C57BL/6 mice were infected as described in the legend for Fig. 1 and analyzed for inflammatory leukocyte populations in livers and spleens. Shown are time courses of changes in populations of iDCs (distinguished as illustrated in Fig. 5) in spleens and livers during infection with parent (filled circles) and Δ*yopM* (open circles) *Y. pestis*. PMNs were gated out by removing CD11b^{+} Ly6G^{+} cells (upper right quadrants of scatter plots for Ly6G versus CD11b in Fig. 1B). The remaining live cells were evaluated for the presence of CD11b (myeloid cells) and CD11c (DCs). iDCs, inflammatory DCs (CD11b^{+} CD11c$^{Lo\text{-}Int}$). The point at time zero indicates the value for uninfected mice. Each datum point represents the average of values from 20 mice. The error bars indicate the standard deviations. Significant differences by unpaired Student's *t* test comparing data from mice infected with the parent and mutant strains are indicated (**, $P < 0.01$).

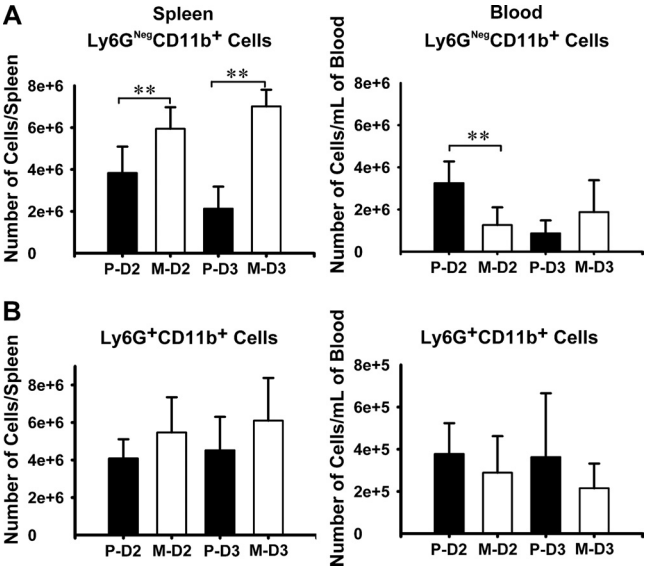

FIG. 8. Inhibition of iMO/iDC recruitment into spleen and into circulation by parent *Y. pestis* KIM5. C57BL/6 mice were infected with parent and Δ*yopM Y. pestis* and analyzed by flow cytometry for populations of live leukocytes in spleen and peripheral blood on days 2 and 3 p.i. (indicated, respectively, as D2 and D3). P, mice infected with the parent strain; M, mice infected with the Δ*yopM* mutant. (A) Ly6G^{-} CD11b^{+} cells, distinguished as illustrated in the lower right quadrants of Fig. 1B. (B) Ly6G^{+} CD11b^{+} cells (PMNs), distinguished as illustrated in the upper right quadrants of Fig. 1B. Each datum point represents the average of values from 9 mice. The error bars indicate the standard deviations. Significant differences by unpaired Student's *t* test comparing data from mice infected with the parent and mutant strains are indicated (**, $P < 0.01$).

through CCR2, and during this process some develop into iDCs (3, 27). Conceivably, the parent *Y. pestis* could influence recruitment of iMOs from bone marrow into the blood, from the blood into infected organs, or both. To gain insight into how the parent *Y. pestis* might control influx of inflammatory cells into spleen, we compared numbers of Ly6G^{+} CD11b^{+} and Ly6G^{-} CD11b^{+} cells in peripheral blood and in spleens from mice infected with parent and Δ*yopM Y. pestis*. These populations contain iMOs and some immature DCs in blood; in spleen, they are iMOs plus iDCs that matured from iMOs in addition to resident Mϕs and myeloid DCs present before infection. To allow comparison of cell numbers between spleen and blood, the data are presented as absolute numbers, rather than percentages, of live cells per organ. Figure 8A shows that, as expected, Ly6G^{-} CD11b^{+} cells showed greater accumulation in spleens of mice infected by the Δ*yopM* mutant than in those of mice infected with the parent *Y. pestis*, and this difference intensified on day 3 compared to day 2 p.i. In blood, the reverse situation held on day 2 p.i.: there were 2.5 times as many Ly6G^{-} CD11b^{+} leukocytes in the blood of mice infected with the parent strain as in the blood of mice infected with the Δ*yopM* mutant strain, while the net numbers of Ly6G^{-} CD11b^{+} cells (summing those in spleen and in the estimated total blood volume) were similar between the two sets of mice (8.2×10^{6} and 9.7×10^{6}, respectively). However, by day 3 p.i., there were almost 4-fold fewer of these cells in the circulation of mice infected by the parent *Y. pestis* than on day 2, and numbers in spleens of these mice had decreased as well. As previously shown (66), there was no significant difference in recruitment of PMNs into spleens by the two strains of *Y. pestis*; there also was no difference in numbers of circulating PMNs in the two sets of infected mice (Fig. 8B).

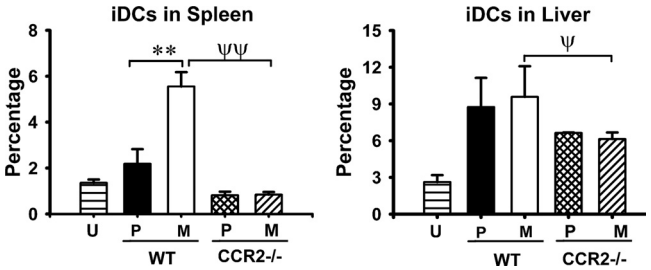

FIG. 7. CCR2 dependence of iDC recruitment. WT and CCR2$^{-/-}$ C57BL/6 mice were infected with parent and Δ*yopM Y. pestis* KIM5 and analyzed as described in the legend for Fig. 6 for iDCs in spleens and livers on day 3. U, uninfected mice; P/WT, WT mice infected with parent *Y. pestis*; M/WT, WT mice infected with Δ*yopM Y. pestis*; P/CCR2$^{-/-}$, CCR2$^{-/-}$ mice infected with the parent strain; M/CCR2$^{-/-}$, CCR2$^{-/-}$ mice infected with the Δ*yopM* strain. Each datum point represents the average of values from 19 mice. The error bars indicate the standard deviations. In comparisons between WT and CCR2$^{-/-}$ groups, ψ, $P < 0.05$, and ψψ, $P < 0.01$, for mice infected with Δ*yopM Y. pestis*; In comparisons between groups of mice infected with parent and Δ*yopM Y. pestis*, **, $P < 0.01$ for WT mice.

These findings suggested that, by day 2 of infection, there was a bottleneck at the level of becoming tissue associated in spleen for iMOs and iDCs in mice infected with parent *Y. pestis* and that the recruitment deficit extended to affect the recruitment into the circulation by day 3 p.i. In contrast, recruitment into spleen was robust during infection by the Δ*yopM* mutant, and recruitment into blood was maintained up to day 3 p.i.

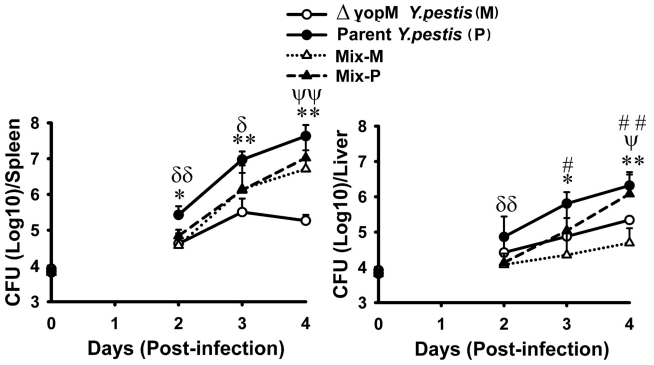

FIG. 9. *trans* complementation of Δ*yopM Y. pestis* KIM5 in spleen but not in liver. C57BL/6 mice were infected i.v. with 5×10^3 CFU Δ*lacZ Y. pestis* KIM5-3003 (parent strain in terms of the *yopM* gene) or Δ*yopM* strain separately or as a 1:1 mixture and analyzed for CFU in spleen and liver on days 2, 3, and 4 p.i. Mix-P, Δ*lacZ* parent strain CFU from mice infected with the mixture; Mix-M, Δ*yopM* mutant CFU from mice infected with the mixture. The points at time zero represent the doses given to the mice. Each datum point represents the average of values from 8 mice. δ, $P < 0.05$, and δδ, $P < 0.01$, for mice infected with Mix-P and P; ψ, $P < 0.05$, and ψψ, $P < 0.01$, for mice infected with Mix-M and M; ∗, $P < 0.05$, and ∗∗, $P < 0.01$, for mice infected with M and P; #, $P < 0.05$, and # #, $P < 0.01$, for mice infected with Mix-M and Mix-P.

Coinfection with parent and Δ*yopM Y. pestis* relieves the growth defect of the Δ*yopM* strain in spleen but not in liver. Based on our findings, we hypothesized that *Y. pestis* that could express YopM and deliver the protein to host cells could prevent the influx of iDCs into spleen, which in turn were critical for controlling growth of Δ*yopM Y. pestis* in that organ. This hypothesis predicted that in spleen, the Δ*yopM* mutant would be protected from growth limitation if the parent strain were present to exert its inhibitory effect on iDC recruitment. We tested this idea by comparing growth of the two strains singly and in a 1:1 mixture in spleens and livers of WT mice. To distinguish the two strains, we deleted the *lacZ* gene in the parent strain and used blue-white screening on agar medium containing X-Gal (5-bromo-4-chloro-3-indolyl-β-D-galactopyranoside), as done by Lawrenz et al. (28). To increase the likelihood of depositing some of each strain in infected splenic and hepatic sinusoids, we used a higher infectious dose than in the experiments so far (5×10^3 CFU). Figure 9 shows that by day 2 p.i., the two *Y. pestis* strains in coinfected spleens showed the same viable numbers as the Δ*yopM* mutant growing separately; thereafter, the YopM-related growth limitation was abolished and the two *Y. pestis* strains grew identically at the rate shown by the parent strain growing separately. In contrast, after day 2 in liver, there was little difference between the growth rates of the bacteria administered separately and together, and the YopM-associated difference in bacterial numbers was maintained between parent and mutant. However, as in spleen, at the initial time point on day 2 p.i. the two *Y. pestis* strains showed the lower growth yield characteristic of the Δ*yopM* mutant. We hypothesize that after day 2 p.i., when the effect of YopM on recruitment of iDCs is manifested, YopM in the parent *Y. pestis* lessened the influx of iDCs into spleen, thereby protecting parent and nearby Δ*yopM* bacteria from the growth-inhibitory effects of these inflammatory cells. In liver, the parent strain promoted only its own growth by a mechanism that did not afford protection to nearby Δ*yopM* bacteria. However, initially in both organs, the proinflammatory effects of the Δ*yopM* mutant were dominant, to the detriment of the parent strain.

Growth of Δ*yopM Y. pestis* in skin is promoted in CCR2$^{-/-}$ mice. We previously showed that YopM is necessary for full lethality of bubonic plague in mice and that at least by 8 h p.i. there is a robust influx of inflammatory cells into skin infected with either parent or Δ*yopM Y. pestis* CO92 (66). In this study, we have seen that CCR2$^+$ cells are essential for mediating growth restriction during systemic plague of Δ*yopM Y. pestis* KIM5 grown at 26°C (Fig. 3). Accordingly, we hypothesized that CCR2$^+$ cells mediate the decreased virulence of Δ*yopM Y. pestis* CO92 in bubonic plague by limiting growth in skin and/or dissemination to spleen. In a pilot experiment, we had found that dissemination of the parent *Y. pestis* CO92.S6 to spleen was detectable in only a few mice on day 2 and day 3 p.i., whereas the Δ*yopM* strain CO92.S19 showed dissemination in only a few mice on day 4 and day 5 p.i. (data not shown). Accordingly, we measured viable numbers in the skin surrounding the infection site and in spleens on days 4 and 5 p.i. in groups of WT and CCR2$^{-/-}$ mice infected i.d. with parent and Δ*yopM Y. pestis* CO92 (Fig. 10). Because Δ*yopM Y. pestis* is only ca. 24-fold less lethal than the parent strain in skin infection (66), the range of doses that would reveal the phenotype due to the absence of YopM while being lethal (significantly greater than the LD_{50}) for the parent strain was narrow. Accordingly, the experiments with results shown in Fig. 10 employed 5 to 10 LD_{50} of the parent strain and 0.5 LD_{50} of the Δ*yopM* mutant. In WT mice, both strains colonized skin; however, Δ*yopM Y. pestis* showed a delay compared to the parent strain. In contrast, the Δ*yopM* strain grew better in the skin of CCR2$^{-/-}$ mice, surpassing even the parent strain in viable numbers on day 5 p.i. There was no difference seen between WT and CCR2$^{-/-}$ mice for the parent strain at day 4 p.i., but by day 5 p.i., 5 of the mice infected with the parent *Y. pestis* had died (indicated by × in Fig. 10). Dissemination to spleen was not affected by the CCR2 knockout on day 4 p.i., but on day 5, there was a trend toward stronger colonization of the spleen by the Δ*yopM* strain in the CCR2$^{-/-}$ mice than by this strain in the WT mice (not statistically significant, $P = 0.09$). These findings suggest that CCR2$^+$ cells play a role in controlling *Y. pestis* bacterial numbers in skin when YopM is absent.

DISCUSSION

YopM is the only effector Yop for which a pathogenic mechanism has not been clearly defined. We are using a systemic plague model to identify the cells responsible for the attenuation of Δ*yopM Y. pestis*. Because YopM's pathogenic mechanism is ultimately directed against these cells, e.g., by inhibiting their recruitment or activity, we can then work back to specific pathways through which YopM likely acts. In this study, we pursued our previous finding that Gr1$^+$ cells selectively limit the growth of Δ*yopM Y. pestis* KIM5 (66).

When PMNs were ablated, growth of Δ*yopM Y. pestis* was disproportionately enhanced in liver compared to that of the parent strain, showing that PMNs are selectively involved in controlling growth of the mutant in that organ. In contrast,

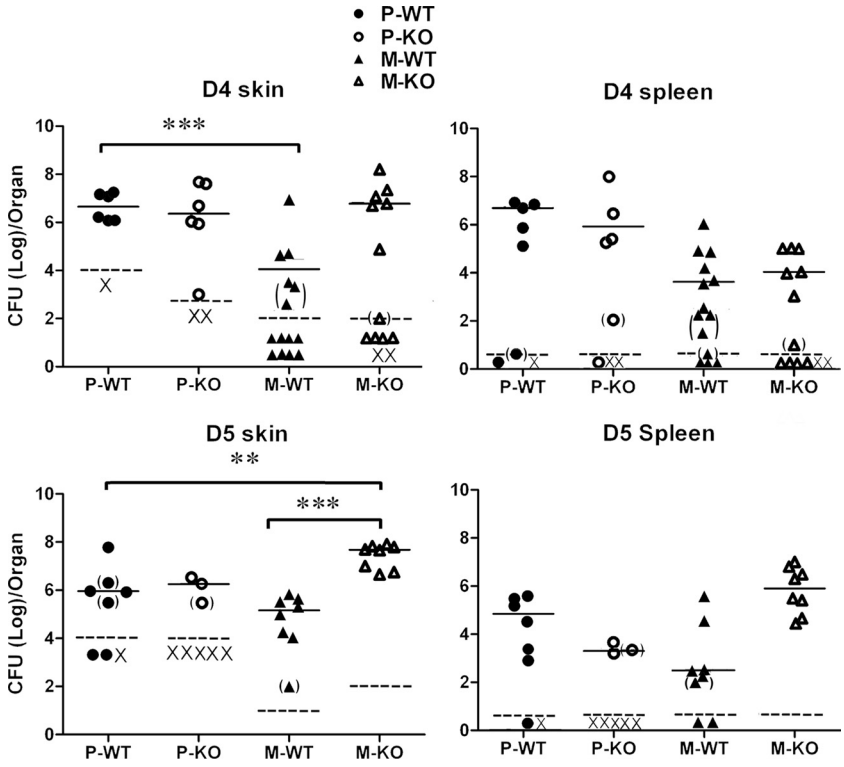

FIG. 10. CCR2 requirement to control local growth of Δ*yopM Y. pestis* CO92 in bubonic plague. Groups of C57BL/6 and CCR2$^{-/-}$ mice were infected i.d. with 100 to 200 CFU of parent *Y. pestis* CO92.S6 or 200 to 250 CFU of Δ*yopM Y. pestis* CO92.S19, and skin and spleens were analyzed for CFU on days 4 and 5 p.i. (D4 and D5, respectively). Because of the large number of mice involved, the infections for the two analysis times were done on different days. To improve the statistical power in the data for the Δ*yopM* mutant on day 4 p.i., that experiment was repeated and the data for the two experiments were pooled. Each symbol represents one mouse. P-WT, parent strain and WT mice (8 mice in the group); M-WT, Δ*yopM* mutant and WT mice (14 mice in the group on day 4 p.i. and 8 mice in the group on day 5 p.i.); P-KO, parent strain and CCR2$^{-/-}$ mice (8 mice in the group); M-KO, Δ*yopM* mutant and CCR2$^{-/-}$ mice (14 mice in the group on day 4 p.i. and 8 mice in the group on day 5 p.i.); ×, mouse died prior to analysis. Solid horizontal lines indicate median values of the data sets, and dashed lines show limits of detection (a single colony on one of the duplicate plates). Parentheses indicate data taken from samples with <30 CFU. Significant differences of medians by the Wilcoxon two-sample test are indicated: **, $P \leq 0.01$; ***, $P \leq 0.001$. On day 5 p.i., the number of P-KO mice that survived to be analyzed was too low for statistical evaluation, and the data for these mice likely underestimate those for the group. One sample of skin from a P-WT mouse on day 5 p.i. was lost, and one sample of spleen from an M-KO mouse on day 4 p.i. could not be enumerated (accounting for one less datum point in those treatment groups).

there was no effect of the ablation on growth of the Δ*yopM* strain in spleen. We had previously shown that there is no difference in recruitment of PMNs to spleen or liver in mice infected with parent or Δ*yopM Y. pestis* (66). Taken together, the findings indicate that YopM directly or indirectly undermines a function of PMNs in liver but that in spleen these cells are not a critical target of YopM's pathogenic mechanism or they are a redundant target.

Often, in inflammatory situations PMNs serve as early responders, and the cytokines and chemokines they produce elicit the influx of MOs as a secondary wave of the inflammatory response (21, 55). However, this does not appear to be the case in a rat model of bubonic plague, where numbers of MOs appeared in primary lymph nodes 18 h before PMN numbers increased, and in spleen, PMNs and MOs were noted to appear at about the same time (47). In our systemic plague model, influx of PMNs and MOs peaks at the same time in both spleen and liver (66), and in the present study, depletion of PMNs did not delay or diminish the influx of Ly6G$^-$ CD11b$^+$ MOs and DCs. These observations indicate that recruitment of MOs in plague is independent of PMNs, raising the potential for pathogen-directed modulation of influx of inflammatory MOs and DCs through pathways not involving PMNs.

We previously observed that Ly6G$^-$ CD11b$^+$ cells (potentially iMOs, Mϕs, iDCs, and myeloid DCs) failed to accumulate stably in spleen in response to infection by the parent *Y. pestis*, in contrast to infection by the Δ*yopM* mutant (66). When Gr1$^+$ cells were ablated, the influx of Ly6G$^-$ CD11b$^+$ cells did not occur, indicating that those cells potentially were inflammatory MOs and DCs. These cells became prime candidates for Gr1$^+$ cells that selectively control growth of Δ*yopM Y. pestis* in spleen once we found that PMNs were not required in that organ. Because these cells largely depend on CCR2 for recruitment to foci of infection, we could test their involvement by comparing growth of parent and mutant *Y. pestis* in CCR2$^{-/-}$ mice. Indeed, spleens of CCR2$^{-/-}$ mice had greatly reduced recruitment of Ly6G$^-$ CD11b$^+$ cells, and the Δ*yopM* mutant grew nearly as well as the parent strain (Fig. 3C), directly implicating cells recruited through CCR2 in controlling growth of Δ*yopM Y. pestis*. We hypothesize that YopM selectively inhibits recruitment of inflammatory MOs and DCs into

spleen; when YopM is absent, those cells accumulate at foci of infection and limit growth of the bacteria.

By days 2 and 3 of infection, the cells differentially recruited into spleen by Δ*yopM* and parent *Y. pestis* were $Gr1^+$ $CD11b^{Int-+}$ $CD11c^{Lo-Int}$ $iNOS^+$ $Mac3^+$ inflammatory DCs (Fig. 5 through 7). These cells develop from MOs that are recruited into circulation in response to infection (3, 51). The nitric oxide (NO) produced by these cells at foci of infection could be responsible for limiting net growth of the Δ*yopM* mutant. Even though the bacteria are predominantly extracellularly located in spleens by day 2 of infection (32), NO can be an effective antibacterial mechanism, as indicated in studies of bubonic and septicemic plague where free NO is available for killing extracellular bacteria and nitrosative stress is a prominent driving force shaping *Y. pestis* gene expression and metabolism (48). The parent *Y. pestis* could decrease its exposure to this antibacterial agent by limiting influx of the NO-producing cells. Consistent with this idea, the presence of the parent strain conferred partial protection on the Δ*yopM* mutant in spleen after day 2 in the coinfection experiment. Interestingly, there was a reciprocal but detrimental effect of the mutant strain on net growth of the parent strain prior to day 3 of infection (Fig. 9). This likely is a distinct phenomenon, as it happened in both liver and spleen. We speculate that resident and early-responding inflammatory cells are stimulated in the focus of infection by proinflammatory cytokines induced in expression by the Δ*yopM* strain (25) and that these cells have heightened antibacterial activity that affects both *Y. pestis* strains in the coinfection.

The parent *Y. pestis* initially exerted its inhibition of recruitment at the level of emigration of iMOs from the blood into spleen (Fig. 8A). As infection progressed, the population of these cells declined even below the basal level present in noninfected mice, indicating that a second process may inhibit or remove the signals that retain iMOs in spleen. In mice infected with the Δ*yopM* mutant but not parent *Y. pestis*, iDCs were recruited and retained by spleen. In contrast, PMNs were captured in similar numbers in spleens infected with the two strains (Fig. 8B). These findings imply that YopM affects recruitment mechanisms in spleen that are distinct between PMNs and iMOs (the circulating precursors of iDCs). The greatest distinction between the two cell types in the recruitment process lies in the chemokines that bind G protein-coupled receptors. This process activates integrins to cause arrest and then migration into tissues to inflammatory sites (8, 31, 39). Two prominent chemokines that selectively elicit migration of monocytes in many systems are CCL2/MCP-1 and CCL5/RANTES, which are produced by cytokine-stimulated platelets, cytokine-activated endothelial cells (ECs), stimulated mast cells, and stimulated resident macrophages (10, 24, 27, 42, 50, 63) as well as stimulated PMNs (55). Additional chemokines not selective for migration of MOs can synergize with CCL2 (e.g., N-formyl-Met-Leu-Phe [fMLP], platelet-activating factor, and CXCL12/stromal cell-derived factor 1) (14). In our studies, the absence of CCR2, the receptor for CCL2/MCP-1, CCL7/MCP-3, and CCL13/MCP-4 (7), was sufficient to relieve the growth defect of Δ*yopM Y. pestis*. CCL2/MCP-1 and CCL7/MCP-3 are known to elicit iMO recruitment in an additive manner during *Listeria* infection (24), and iDCs, which we found to be selectively accumulated in spleens infected with Δ*yopM Y. pestis*, are defective for recruitment to spleen in $CCR2^{-/-}$ mice (40). YopM could indirectly influence production of chemokines that signal through CCR2 in spleen by downregulating expression of cytokines, such as IL-1β and TNF-α (25), that activate ECs (33, 45) or by directly downregulating a cell biological pathway that leads to chemokine expression.

Some conflicting findings have come from two recent investigations using different strains of *Y. pseudotuberculosis* grown at ambient temperature. Both studies were pursuing the finding by McDonald et al. (35) that YopM can bind and activate two serine/threonine kinases, PRK2 and RSK1. McPhee et al. (36) noted a decrease in splenic iMOs ($Ly6G^-$ $Ly6C^+$ $CD11b^+$ cells) on day 4 p.i. in C57BL/6 mice infected i.v. with the YopM-deleted strain of *Y. pseudotuberculosis* compared to the level in mice infected with the parent. In contrast, McCoy et al. (34) found that C57BL/6 mice infected i.v. by a Δ*yopM* strain of *Y. pseudotuberculosis* elicited more splenic iMOs than did infection with parent *Y. pseudotuberculosis* on day 4 p.i. The two studies also differed in whether the presence of YopM in the infecting strain correlated with increased numbers of PMNs recruited to spleen (34) or had no significant effect on PMN recruitment (36). Future work is needed to determine if the differences between these two studies are due to the use of different *Y. pseudotuberculosis* strains. Further, because of numerous differences in surface molecules expressed by *Y. pseudotuberculosis* and *Y. pestis* grown at 26°C (e.g., the former has flagella and the latter does not), the cell biological contexts in which YopM acts are different in infections by the two *Yersinia* species. However, the studies by McCoy et al. and McPhee et al. agreed that the ability of YopM to bind RSK1 contributes to virulence of *Y. pseudotuberculosis*, and it is noteworthy that *Y. pestis* YopM does bind RSK1 (34, 35; unpublished data). We do not yet know whether this interaction is involved in the chemokine pathways in spleen discussed earlier.

Liver structure, function, and response to infection are distinct from those in spleen (23, 40). In liver sinusoids, Kupffer cells (KCs) and neutrophil-KC interactions are prominent in the response to bacterial infection (16, 17, 20). KCs themselves are not potent antibacterial cells, but they bind bacteria avidly and present them to PMNs for killing (15–17, 29). In response to stimulation of Toll-like receptors (TLRs), KCs do produce IL-1β, IL-6, and TNF-α (16), which activate ECs to produce CCL2/MCP-1. KCs also produce CCL3/macrophage inflammatory protein 1α (MIP-1α), which recruits DC precursors to liver (67).

Liver has not been studied as much as spleen for its response to *Yersinia* infection. In our systemic plague studies, we found that in contrast to spleen, liver did not respond with differential iDC recruitment in mice infected with parent and Δ*yopM Y. pestis* (Fig. 6), and the parent strain did not complement the Δ*yopM* mutant in *trans* after day 2 p.i. These findings suggest that YopM does not exert a dominant effect on chemokine pathways in liver or, alternatively, that YopM's effect on chemokine pathways is redundant for recruitment of inflammatory cells. This idea is consistent with our previous findings that spleen and liver respond to *Y. pestis* infection differently with regard to recruitment of NK cells and plasmacytoid DCs as well as $Ly6G^-$ $CD11b^+$ cells (66). The critical importance of

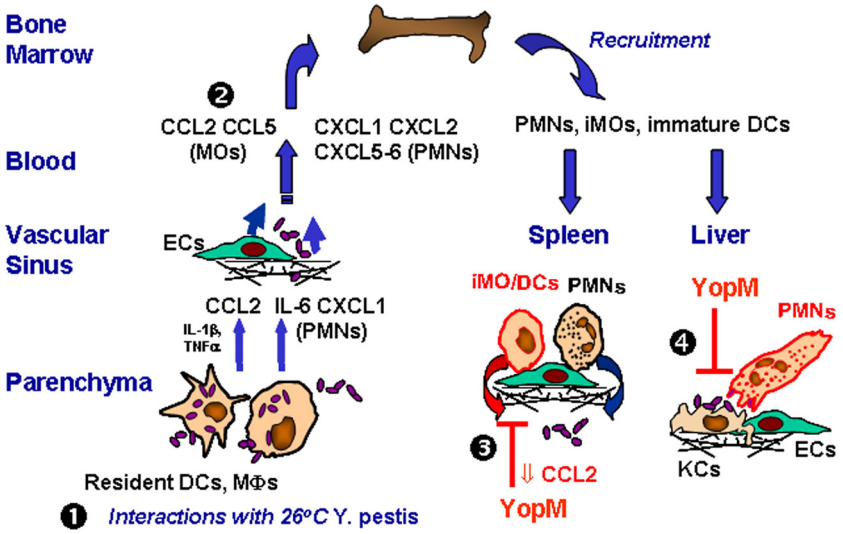

FIG. 11. Model for how YopM affects cells and cytokines in systemic plague caused by *Y. pestis.* The flow of events following i.v. infection of WT mice is indicated by the numbers. At step 1, the bacteria have seeded liver and spleen and are interacting with resident cells. Red coloration denotes YopM-specific effects. See the Discussion for a narrative description.

CCR2 for recruitment of cells into spleen but not liver during systemic plague and a selective inhibitory effect of YopM$^+$ *Y. pestis* on this recruitment may explain our previous finding that NK cells, which are recruited via CCR2, are differentially recruited to spleen by the parent and Δ*yopM* strains, whereas there is no difference in recruitment of NK cells by the two *Y. pestis* strains in liver (25, 66).

Nonetheless, Gr1$^+$ cells dependent on CCR2 function were required to control growth of the Δ*yopM* mutant in liver (66) (Fig. 3C). We have identified PMNs as critical cells that control growth of Δ*yopM Y. pestis* in liver. These cells are Gr1$^+$, and half of the PMNs in livers of mice infected with Δ*yopM Y. pestis* are CCR2$^+$ (data not shown). However, the role of CCR2 in PMN function is unclear (22). This chemokine receptor does promote PMN differentiation and adherence (22, 27) and can stimulate PMN antibacterial activities (18). During capture of PMNs from circulation, chemokines bound to proteoglycans on ECs (31, 65) might signal through CCR2 and promote subsequent PMN antibacterial function. Alternatively, CCR2 on KCs might be critical for the antibacterial collaboration with PMNs to be productive. Consistent with these speculations, even though CCR2$^-$ mice responded to infection by Δ*yopM Y. pestis* with enhanced recruitment of PMNs (Fig. 3B), these PMNs apparently were not functional, because the Δ*yopM* mutant grew better in these mice than in WT mice, in which fewer PMNs were present in organs (Fig. 3C). In the coinfection experiment, it is unlikely that parent and mutant yersiniae would bind to the same KC, and KCs that bind *Y. pestis* that lacks YopM retain their ability to present CCR2-binding chemokines to PMNs, which in turn could kill some of the bacteria. Meanwhile, the parent *Y. pestis* on nearby KCs protects itself from PMN antibacterial activity, and the parent strain maintains its growth advantage over the Δ*yopM* mutant after day 2 p.i.

In our studies, *Y. pestis* was grown at ambient temperature so that the host responses would include those elicited by the characteristic surface composition of such bacteria and might resemble those in skin during bubonic plague. Because CCR2 function was critical for limiting growth of the Δ*yopM* mutant in both liver and spleen, we hypothesized that this would also be the case when mice were challenged i.d. with ambient-temperature-grown *Y. pestis*. Indeed, the Δ*yopM Y. pestis* strain CO92.S19 showed delayed growth in skin compared to that of the fully virulent parent *Y. pestis* CO92.S6 in WT mice at day 4 p.i. (Fig. 10, top). Further, the Δ*yopM* mutant grew as well in CCR2$^{-/-}$ mice as the parent strain did in skin of WT mice. As seen in liver and spleen in systemic plague, growth of the parent strain in skin was not altered in the CCR2$^{-/-}$ mice compared to that in WT mice, likely because YopM was present to neutralize CCR2-related functions in WT mice. Therefore, our findings show that signals through CCR2 are important for defense against both bubonic and systemic plague.

Figure 11 incorporates the findings of this study in a model for the sequence of events in systemic plague of WT mice. As shown by step 1, the input ambient-temperature-grown yersiniae reach the discontinuous endothelium of liver and spleen via the blood and interact with resident DCs and Mϕs (KCs in liver). Initially, their lipid A is hexa-acylated and stimulates TLR4 (38, 43) on resident cells, creating a local proinflammatory environment. The yersiniae also initially do not express their thermally induced antiphagocytic properties, such as the T3SS, Caf1, and PsaA, but have adhesins, such as Pla and Ail. Through these, the yersiniae can bind to resident Mϕs and DCs, be engulfed, and potentially promote proinflammatory cytokine expression through stimulation of intracellular molecular pattern receptors, such as NOD1 and NOD2 (52). Once released, however, the yersiniae are fully adapted to 37°C and able to resist phagocytosis by PMNs. As shown by step 2, the initial proinflammatory condition attracts PMNs and inflammatory MOs/DCs from blood and recruits more of these cells from the bone marrow. They are recruited in parallel, through separate chemokine pathways. PMNs are recruited similarly whether YopM is present or absent from the infecting

Y. pestis. Therefore, YopM does not likely have a major effect on the initial capture and rolling steps mediated on ECs by selectins that interact with both PMNs and iMOs. As shown by step 3, however, YopM delivered to resident cells by extracellular *Y. pestis* curtails expression of proinflammatory cytokines and some chemokines that until then were activating cells locally and providing a beacon for iMOs to home toward. The result is decreased numbers of iDCs in spleens of mice infected with parent *Y. pestis*. If the infecting *Y. pestis* strain lacks YopM, iMOs develop into iDCs that persist in spleen and may reduce net growth of the bacteria by releasing NO. As shown by step 4, in liver, recruitment of iDCs is not selectively affected by YopM, but in some way PMN function is undermined, perhaps indirectly at the level of an interaction of PMNs with KCs that have received YopM. If YopM is not present in the infecting strain, PMNs are thought to reduce net growth of the bacteria through production of bactericidal compounds, including reactive oxygen species and defensins.

In conclusion, this study has identified CCR2 as a critical node in the chemokine communication network with which YopM interfaces for its pathogenic effect: when mice lack CCR2, Δ*yopM Y. pestis* grows almost as well as the parent strain. This finding provides a framework for focusing future research to identify YopM's direct molecular targets. The cellular dynamics through which CCR2 functions differ in liver and spleen, with YopM disabling the recruitment of $CCR2^+$ $Gr1^+$ iDCs into spleen, whereas in liver, it is the function of $Gr1^+$ PMNs that is undermined, and CCR2 is necessary for activity of the PMNs or of cells, such as KCs, that interact with PMNs in the control of bacterial proliferation. Importantly, CCR2 also was found to be responsible for controlling growth of Δ*yopM Y. pestis* in skin, indicating that YopM's molecular targets in skin ultimately influence signaling through CCR2 and showing that CCR2-mediated functions are important in host defense against bubonic plague.

ACKNOWLEDGMENTS

This study was supported by Public Health Service grant R01AI67869 from the National Institute for Allergy and Infectious Diseases. Z.Y. was supported by a Dissertation Year Fellowship and a Presidential Fellowship from the University of Kentucky.

We gratefully acknowledge excellent technical help with animal experiments from Amanda A. Gorman and Tanya Myers-Morales. We appreciate the help of Greg Baumann and Jennifer Strange, who processed the flow cytometry samples, and the University of Kentucky for its support of the Flow Cytometry Core Facility. We thank Robinette King for her guidance on raising the $CCR2^{-/-}$ mice.

REFERENCES

1. **Achtman, M., et al.** 2004. Microevolution and history of the plague bacillus, Yersinia pestis. Proc. Natl. Acad. Sci. U. S. A. **101:**17837–17842.
2. **Ambati, J., et al.** 2003. An animal model of age-related macular degeneration in senescent Ccl-2- or Ccr-2-deficient mice. Nat. Med. **9:**1390–1397.
3. **Auffray, C., et al.** 2009. CX_3CR1^+ $CD115^+$ $CD135^+$ common macrophage/DC precursors and the role of CX_3CR1 in their response to inflammation. J. Exp. Med. **206:**595–606.
4. **Bobrov, A. G., and R. D. Perry.** 2006. *Yersinia pestis lacZ* expresses a β-galactosidase with low enzymatic activity. FEMS Microbiol. Lett. **255:**43–51.
5. **Boring, L., et al.** 1997. Impaired monocyte migration and reduced type I (Th1) cytokine responses in C-C chemokine receptor 2 knockout mice. J. Clin. Invest. **100:**2552–2561.
6. **Burnett, S. H., et al.** 2004. Conditional macrophage ablation in transgenic mice expressing a Fas-based suicide gene. J. Leukoc. Biol. **75:**612–623.
7. **Chensue, S. W.** 2001. Molecular machinations: chemokine signals in host-pathogen interactions. Clin. Microbiol. Rev. **14:**821–835.
8. **Cook-Mills, J. M., and T. L. Deem.** 2005. Active participation of endothelial cells in inflammation. J. Leukoc. Biol. **77:**487–495.
9. **Daley, J. M., A. A. Thomay, M. D. Connolly, J. S. Reichner, and J. E. Albina.** 2008. Use of Ly6G-specific monoclonal antibody to deplete neutrophils in mice. J. Leukoc. Biol. **83:**64–70.
10. **Deshmane, S. L., S. Kremlev, S. Amini, and B. E. Sawaya.** 2009. Monocyte chemoattractant protein-1 (MCP-1): an overview. J. Interferon Cytokine Res. **29:**313–326.
11. **Egan, C. E., W. Sukhumavasi, A. L. Bierly, and E. Y. Denkers.** 2008. Understanding the multiple functions of $Gr\text{-}1^+$ cell subpopulations during microbial infection. Immunol. Res. **40:**35–48.
12. **Forman, S., et al.** 2008. yadBC of Yersinia pestis, a new virulence determinant for bubonic plague. Infect. Immun. **76:**578–587.
13. **Geissmann, F., S. Jung, and D. R. Littman.** 2003. Blood monocytes consist of two principal subsets with distinct migratory properties. Immunity **19:**71–82.
14. **Gouwy, M., et al.** 2008. Synergy between coproduced CC and CXC chemokines in monocyte chemotaxis through receptor-mediated events. Mol. Pharmacol. **74:**485–495.
15. **Gregory, S. H., A. J. Sagnimeni, and E. J. Wing.** 1996. Bacteria in the blood are trapped in the liver and killed by immigrating neutrophils. J. Immunol. **157:**2514–2520.
16. **Gregory, S. H., and E. J. Wing.** 2002. Neutrophil-Kupffer cell interaction: a critical component of host defenses to systemic bacterial infections. J. Leukoc. Biol. **72:**239–248.
17. **Gregory, S. H., et al.** 2002. Complementary adhesion molecules promote neutrophil-Kupffer cell interaction and the elimination of bacteria taken up by the liver. J. Immunol. **168:**308–315.
18. **Hartl, D., et al.** 2008. Infiltrated neutrophils acquire novel chemokine receptor expression and chemokine responsiveness in chronic inflammatory lung diseases. J. Immunol. **181:**8053–8067.
19. **Heusipp, G., K. Spekker, S. Brast, S. Fälker, and M. A. Schmidt.** 2006. YopM of *Yersinia enterocolitica* specifically interacts with alpha 1-antitrypsin without affecting the anti-protease activity. Microbiology **152:**1327–1335.
20. **Holub, M., et al.** 2009. Neutrophils sequestered in the liver suppress the proinflammatory response of Kupffer cells to systemic bacterial infection. J. Immunol. **183:**3309–3316.
21. **Hurst, S. M., et al.** 2001. IL-6 and its soluble receptor orchestrate a temporal switch in the pattern of leukocyte recruitment seen during acute inflammation. Immunity **14:**706–714.
22. **Iida, S., T. Kohro, T. Kodama, S. Nagata, and R. Fukunaga.** 2005. Identification of CCR2, flotillin, and gp49B genes as new G-CSF targets during neutrophilic differentiation. J. Leukoc. Biol. **78:**481–490.
23. **Ishibashi, H., M. Nakamura, A. Komori, K. Migita, and S. Shimoda.** 2009. Liver architecture, cell function, and disease. Semin. Immunopathol. **32:**399–409.
24. **Jia, T., et al.** 2008. Additive roles for MCP-1 and MCP-3 in CCR2-mediated recruitment of inflammatory monocytes during *Listeria monocytogenes* infection. J. Immunol. **180:**6846–6853.
25. **Kerschen, E. J., D. A. Cohen, A. M. Kaplan, and S. C. Straley.** 2004. The plague virulence protein YopM targets the innate immune response by causing a global depletion of NK cells. Infect. Immun. **72:**4589–4602.
26. Reference deleted.
27. **Kuziel, W. A., et al.** 1997. Severe reduction in leukocyte adhesion and monocyte extravasation in mice deficient in C-C chemokine receptor 2. Proc. Natl. Acad. Sci. U. S. A. **94:**12053–12058.
28. **Lawrenz, M. B., J. D. Lenz, and V. L. Miller.** 2009. A novel autotransporter adhesin is required for efficient colonization during bubonic plague. Infect. Immun. **77:**317–326.
29. **LePay, D. A., C. F. Nathan, R. M. Steinman, H. W. Murray, and Z. A. Cohn.** 1985. Murine Kupffer cells mononuclear phagocytes deficient in the generation of reactive oxygen intermediates. J. Exp. Med. **161:**1079–1096.
30. **Leung, K. Y., B. S. Reisner, and S. C. Straley.** 1990. YopM inhibits platelet aggregation and is necessary for virulence of Yersinia pestis in mice. Infect. Immun. **58:**3262–3271.
31. **Ley, K., C. Laudanna, M. I. Sybulsky, and S. Nourshargh.** 2007. Getting to the site of inflammation: the leukocyte adhesion cascade updated. Nat. Rev. **7:**678–689.
32. **Lukaszewski, R. A., et al.** 2005. Pathogenesis of Yersinia pestis infection in BALB/c mice: effects on host macrophages and neutrophils. Infect. Immun. **73:**7142–7150.
33. **Mantovani, A., C. Garlanda, M. Introna, and A. Vecchi.** 1990. Regulation of endothelial cell function by pro- and anti-inflammatory cytokines. Transplant. Proc. **30:**4239–4243.
34. **McCoy, M. W., M. L. Marré, C. F. Lesser, and J. Mecsas.** 2010. The C-terminal tail of *Yersinia* YopM is critical for interacting with RSK1 and for virulence. Infect. Immun. **78:**2584–2598.
35. **McDonald, C., P. O. Vacratsis, J. B. Bliska, and J. E. Dixon.** 2003. The yersinia virulence factor YopM forms a novel protein complex with two cellular kinases. J. Biol. Chem. **278:**18514–18523.
36. **McPhee, J. B., P. Mena, and J. B. Bliska.** 1 June 2010. Delineation of regions of the *Yersinia* YopM protein required for interaction with the RSK1 and PRK2 host kinases and their requirement for interleukin-10 production and virulence. Infect. Immun. doi:10.1128/IAI.00269-10.

37. **Miller, J. H.** 1972. Experiments in molecular genetics. Cold Spring Harbor Laboratory, Cold Spring Harbor, NY.
38. **Montminy, S. W., et al.** 2006. Virulence factors of *Yersinia pestis* are overcome by a strong lipopolysaccharide response. Nature **7:**1017–1019.
39. **Muller, W. A.** 2003. Leukocyte-endothelial cell interactions in leukocyte transmigration and the inflammatory response. Trends Immunol. **24:**326–333.
40. **Nemeth, E., A. W. Baird, and C. O'Farrelly.** 2009. Microanatomy of the liver immune system. Semin. Immunopathol. **31:**333–343.
41. **Osterholzer, J. J., et al.** 2008. CCR2 mediates conventional dendritic cell recruitment and the formation of bronchovascular mononuclear cell infiltrates in the lungs of mice infected with *Cryptococcus neoformans*. J. Immunol. **181:**610–620.
42. **Øynebråten, I., O. Bakke, P. Brandtzaeg, F.-E. Johansen, and G. Haraldsen.** 2004. Rapid chemokine secretion from endothelial cells originates from 2 distinct compartments. Blood **104:**314–320.
43. **Perry, R. D., and J. D. Fetherston.** 1997. Yersinia pestis—etiologic agent of plague. Clin. Microbiol. Rev. **10:**35–66.
44. Reference deleted.
45. **Rollins, B. J., T. Yoshimura, E. J. Leonard, and J. S. Pober.** 1990. Cytokine-activated human endothelial cells synthesize and secrete a monocyte chemoattractant, MCP-1/JE. Am. J. Pathol. **136:**1229–1233.
46. **Ruter, C., C. Buss, J. Scharnert, G. Heusipp, and M. A. Schmidt.** 2010. A newly identified bacterial cell-penetrating peptide that reduces the transcription of pro-inflammatory cytokines. J. Cell Sci. **123:**2190–2198.
47. **Sebbane, F., D. Gardner, D. Long, B. B. Gowen, and B. J. Hinnebusch.** 2005. Kinetics of disease progression and host response in a rat model of bubonic plague. Am. J. Pathol. **166:**1427–1439.
48. **Sebbane, F., et al.** 2006. Adaptive response of Yersinia pestis to extracellular effectors of innate immunity during bubonic plague. Proc. Natl. Acad. Sci. U. S. A. **103:**11766–11771.
49. **Serbina, N. V., and E. Pamer.** 2006. Monocyte emigration from bone marrow during bacterial infection requires signals mediated by chemokine receptor CCR2. Nat. Immunol. **7:**311–317.
50. **Serbina, N. V., T. Jia, T. M. Hohl, and E. G. Pamer.** 2008. Monocyte-mediated defense against microbial pathogens. Annu. Rev. Immunol. **26:**421–452.
51. **Serbina, N. V., T. P. Salazar-Mather, C. A. Biron, W. A. Kuziel, and E. G. Pamer.** 2003. TNF/iNOS-producing dendritic cells mediate innate immune defense against bacterial infection. Immunity **19:**59–70.
52. **Shaw, M. H., T. Reimer, Y. G. Kim, and G. Nuñez.** 2008. NOD-like receptors (NLRs): bona fide intracellular microbial sensors. Curr. Opin. Immunol. **20:**377–382.
53. **Skrzypek, E., C. Cowan, and S. C. Straley.** 1998. Targeting of the Yersinia pestis YopM protein into HeLa cells and intracellular trafficking to the nucleus. Mol. Microbiol. **30:**1051–1065.
54. Reference deleted.
55. **Soehnlein, O., L. Lindbom, and C. Weber.** 2009. Mechanisms underlying neutrophil-mediated monocyte recruitment. Blood **114:**4613–4623.
56. **Spinner, J. L., J. A. Cundiff, and S. D. Kobayashi.** 2008. Yersinia pestis type III secretion system-dependent inhibition of human polymorphonuclear leukocyte function. Infect. Immun. **76:**3754–3760.
57. **Sunderkötter, C., et al.** 2004. Subpopulations of mouse blood monocytes differ in maturation stage and inflammatory response. J. Immunol. **172:**4410–4417.
58. **Surgalla, M. J., and E. D. Beesley.** 1969. Congo red-agar plating medium for detecting pigmentation in Pasteurella pestis. Appl. Microbiol. **18:**834–837.
59. **Trosky, J. E., A. D. Liverman, and K. Orth.** 2008. Yersinia outer proteins: Yops. Cell. Microbiol. **10:**557–565.
60. **Une, T., and R. R. Brubaker.** 1984. In vivo comparison of avirulent Vwa- and Pgm- or Pstr phenotypes of yersiniae. Infect. Immun. **43:**895–900.
61. **Van Damme, J., P. Proost, J.-P. Lenaerts, and G. Opdenakker.** 1992. Structural and functional identification of two human, tumor-derived monocyte chemotactic proteins (MCP-2 and MCP-3) belonging to the chemokine family. J. Exp. Med. **176:**59–65.
62. **Viboud, G. I., and J. B. Bliska.** 2005. *Yersinia* outer proteins: role in modulation of host cell signaling responses and pathogenesis. Annu. Rev. Microbiol. **59:**69–89.
63. **von Hundelshausen, P., F. Petersen, and E. Brandt.** 2007. Platelet-derived chemokines in vascular biology. Thromb. Haemost. **97:**704–713.
64. **Walunas, T. L., D. S. Bruce, L. Dustin, D. Y. Loh, and J. A. Bluestone.** 1995. Ly-6C is a marker for memory $CD8^+$ T cells. J. Immunol. **155:**1873–1883.
65. **Wang, L., M. Fuster, P. Sriramarao, and J. D. Esko.** 2005. Endothelial heparan sulfate deficiency impairs L-selectin- and chemokine-mediated neutrophil trafficking during inflammatory responses. Nat. Immunol. **6:**901–910.
66. **Ye, Z., et al.** 2009. $Gr1^+$ cells control growth of YopM-negative *Yersinia pestis* during systemic plague. Infect. Immun. **77:**3791–3806.
67. **Yoneyama, H., and T. Ichida.** 2005. Recruitment of dendritic cells to pathologic niches in inflamed liver. Med. Mol. Morphol. **38:**136–141.

Editor: A. J. Bäumler